Continuous Quantification of Spectral Coherence Using Quadratic Time-Frequency Distributions: Error Analysis and Application

M Orini[1,2,3], R Bailón[1,2], LT Mainardi[3], A Mincholé[1,2], P Laguna[1,2]

[1]GTC, Aragón Institute of Engineering Research, University of Zaragoza, Zaragoza, Spain
[2]CIBER de Bioingeniería, Biomateriales y Nanomedicina (CIBER-BBN)
[3]Department of Biomedical Engineering, Politecnico di Milano, Italy

Abstract

Quadratic time-frequency (TF) distributions have an excellent joint TF resolution, but their applicability is limited by the presence of interferences. In this communication, a methodology for robustly estimating TF coherence (TFC), based on signal-dependent smoothing of the Wigner Ville distribution, is shown to provide a reliable continuous quantification of cardiovascular interactions during non stationary conditions. Bias, standard deviation and tracking capability of the TFC estimator have been quantified in different physiological contexts. Linear coupling between HRV and SPV during tilting has been assessed. It is observed that orthostatic stress provokes a significant increase ($p \leq 0.02$) of TFC in both LF and HF range.

1. Introduction

Spectral coherence has been widely applied to quantify the strength of linear relationship between two signals. This measure, being defined in the frequency domain, can not assess the time evolution of the coupling and it is not appropriate for studying non stationary signals. To assess the time evolution of linear coupling an extension of spectral coherence in time-frequency (TF) domain is necessary. Thanks to their excellent joint TF resolution, quadratic TF distributions (QTFD) represent a very powerful tool for studying non stationary signals, and they have been widely applied to the assessment of autonomic nervous modulation [1]. Theoretical properties of TF coherence (TFC) defined using QTFD have been first described in [2], but, to our knowledge, it has never been used in biomedical application. It is defined as:

$$\gamma(t,f) = \frac{C_{1,2}(t,f)C_{1,2}^*(t,f)}{C_1(t,f)C_2(t,f)} \qquad (1)$$

where $C_{1,2}(t,f)$ is the cross TF spectrum and $C_1(t,f)$ and $C_2(t,f)$ are the QTFD of signals $x_1(t)$ and $x_2(t)$, respec-

tively. The unavoidable presence of interference terms (ITs), whose geometry depends on the TF structure of the signals, is the main problem for the definition of a consistent TFC estimator, which should be one (zero) for perfect (lack of) linear coupling, based on QTFD. The main purpose of this communication is to present a consistent estimator of TFC, based on signal-dependent QTFD and bounded in TF regions of interest. To evaluate the estimator accuracy, bias, standard deviation and tracking capability are evaluated through simulations involving non stationary time series which mimic real autonomic signals with known and controlled theoretical coupling. Real data application aiming at monitoring the autonomic response to orthostatic stress is also presented. The time evolution of the coupling between heart rate variability (HRV) and systolic pressure variability (SPV) has been continuously estimated before, during and after upright tilt testing in 15 healthy subjects, allowing to track the dynamics involved in autonomic regulation.

2. Methodology and materials

2.1. Quadratic TF distributions

In this work, a smoothed version of the Wigner Ville distribution (WVD) is used in order to reduce ITs. Smoothing is performed as a 2D convolution between the WVD and a 2D kernel (defined in TF plane). These QTFD can be interpreted as the 2D Fourier transform of a weighted version of the Ambiguity Function (AF) of the signal to be analyzed [3]. The cross-TF spectrum can be defined as:

$$C_{1,2}(t,f;\phi) = W_{1,2}(t,f) \otimes \phi(t,f) = F_{\substack{\tau \to f \\ \nu \to t}}\left\{A_{1,2}(\nu,\tau)\Phi(\nu,\tau)\right\}$$

$$A_{1,2}(\nu,\tau) = F_{t \to \nu}\left\{x_1(t+\frac{\tau}{2})x_2^*(t-\frac{\tau}{2})\right\} \qquad (2)$$

$$\Phi(\nu,\tau) = F_{\substack{t \to \nu \\ f \to \tau}}\left\{\phi(t,f)\right\}$$

where $\otimes$ is the 2D convolution on t and f, $F_{\substack{t \to \nu \\ f \to \tau}}$ is the 2D Fourier Transform operator, used to pass from TF domain to AF domain, and $A_{1,2}(\nu,\tau)$ is the cross-AF of signals $x_1(t)$

and $x_2(t)$. The weighting (smoothing) function $\Phi(\nu, \tau)$ ($\phi(t, f)$) performs as a 2D low pass filter which should be tuned in order to find the better trade-off between ITs suppression and joint TF resolution or, dually, between cross-components suppression and auto-terms concentration (in AF domain). Here, an elliptical exponential kernel, able to automatically adjusts to the TF structure of the signal, is used:

$$\Phi(\nu, \tau; \nu_0, \tau_0, \lambda) = exp\left\{-\pi\left[\left(\frac{\nu}{\nu_0}\right)^2 + \left(\frac{\tau}{\tau_0}\right)^2\right]^{2\lambda}\right\} \quad (3)$$

The kernel's iso-contours are ellipsis, ν_0 and τ_0 affect the length of the axes (the bandwidth of the 2D low pass filter) whereas λ sets its roll off.

2.2. Signal-dependent smoothing

Signals affected by the autonomic modulation may be modeled as the sum of complex exponentials showing both amplitude (AM) and frequency (FM) modulation, embedded in noise. In this study two exponentials are considered to model an AM LF and a AM-FM HF components:

$$x(t) = A_{LF}(t)e^{i\phi_{LF}(t)} + A_{HF}(t)e^{i\phi_{HF}(t)} + \xi(t) \quad (4)$$

where instantaneous frequency is $F(t) = (d\phi(t)/dt)/(2\pi)$. The QTFD of these kinds of signals are expected to present both outer and inner ITs [4]. In order to suppress outer ITs, which mainly oscillate in time direction with a frequency which locally depends on the frequency lag $\nu_i = F_{HF} - F_{LF}$, the kernel should be able to filter out all $\nu > \nu_{i,min}$, where $\nu_{i,min}$ corresponds to the slowest ITs. To obtain $\nu_{i,min}$, the estimation of F_{LF} and $F_{HF}(t)$ is required. A direct or indirect estimation of respiratory rate can be used for approximating $F_{HF}(t)$. For F_{LF} detection, which in the AF results to be concentrated along a line, the Hough Transform (HT) is applied to $|A(\nu, \tau)|$. Due to the hermitian symmetry of the AF, HT can be performed just on $(\nu, \tau) > 0$ resulting faster than in TF domain. The parameter ν_0 in (3) is fixed imposing that $\Phi(\nu_{i,min}, 0; \nu_0, \tau_0, \lambda) = k << 1$, and:

$$\nu_0 = \nu_{i,min}\left(\frac{-log(k)}{\pi}\right)^{-\frac{1}{4\lambda}} \quad (5)$$

In order to find a τ_0, which mainly affects frequency smoothing, which provides a good compromise between ITs suppression (TFC consistency) and TF resolution, an iterative process is proposed. The parameter τ_0 is gradually reduced (increasing smoothing) until $\gamma(t, f)$ achieves full consistency in the TF region of interest. A comprehensive example is shown in Fig 1. Figures 1a-1b represent the case of insufficient smoothing. Outer ITs are still present at midway between the two components and, as expected, they are higher where the two signal spectral components
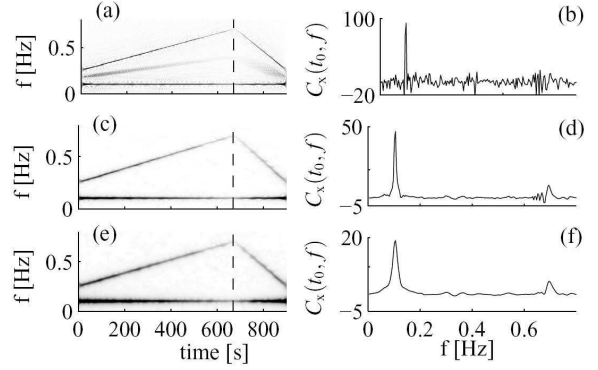

Figure 1. Left: auto TF spectrum $C_x(t, f)$; $x(t)$ components are described in (4) and SNR=5dB; Right: $C_x(t_0, f)$, with t_0 marked by a dotted line in the left panels.
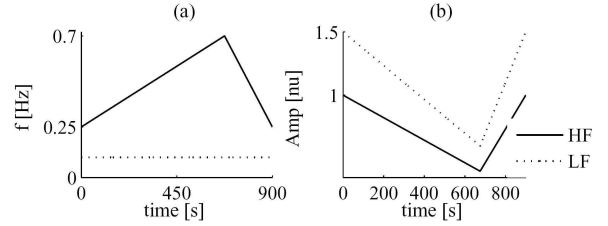

Figure 2. simulation: components of $x(t)$

are closer. In Fig. 1c -1d the TF map computed with the optimized ν_0 is shown. It is free from outer ITs but not from inner ones (see Fig. 1d around 0.6 Hz). Finally, in Fig. 1e-1f, the τ_0 which makes TFC consistent is used.

2.3. Time-Frequency region of interest

The restriction of the TF support of $\gamma(t, f)$ to a region of interest is justified by the desire of finding a good compromise between TF resolution and TFC consistency (full suppression of ITs). The TF region of interest is then defined as the region $\Omega(t, f)$ where

$$\forall t, \ \ C(t, f) > a \cdot \max_f[C(t, f)] \quad (6)$$

with $a < 1$ and $\Omega(t, f) = \Omega_x(t, f) \cap \Omega_y(t, f)$. From $\gamma(t, f)$, defined in $\Omega(t, f)$, the band coherence $\gamma_{B(t)}(t)$ is extracted by averaging in a TV frequency band $B(t)$. In addition, a mean spectral coherence $\gamma(f)$ (generally different from traditional spectral coherence) is retrieved averaging TFC on time.

2.4. Simulation to assess accuracy

The bias, standard deviation and tracking capability of band coherence estimation have been assessed by means of synthetic signals characterized by known and controlled

theoretical coupling. Pairs of signals $[x_1(t), x_2(t)]$ are created adding uncorrelated noises to an original signal $x(t)$: $x_1(t) = x(t) + \xi_1(t)$; $x_2(t) = x(t) + \xi_2(t)$, where $\xi_i(t) = \sigma_i(t)\eta_i(t)$, and $\eta_i(t)$, with $i=[1,2]$, are two zero mean white gaussian noises of variance $\sigma_1^2(t)$ and $\sigma_2^2(t)$, respectively. Imposing $\sigma_1(t)=\sigma_2(t)=\sigma(t)$, theoretical TFC is derived from (1):

$$\gamma_0(t,f) = \frac{C_x^2(t,f)}{C_x^2(t,f) + 2C_x(t,f)C_\xi(t,f;\sigma) + C_\xi^2(t,f;\sigma)} \quad (7)$$

where $C_x(t,f)$ is the QTFD of $x(t)$ and $C_\xi(t,f;\sigma)$ is the QTFD of $\xi_1(t)$ and $\xi_2(t)$. The $\sigma(t)$ corresponding to a given theoretical band coherence $\gamma_{0,B}(t)$, where $B(t)$ is the spectral band of interest, have been obtained by properly integrating (7). Specific situations, aiming at evaluating the performance of the estimator in different physiological contexts, have been modeled using (4):

I) $\gamma_{0,B}(t)$ is constant over time: *a)* $x(t)$ is a white noise. *b)* $x(t)$ mimics a respiratory signal during stress testing: components are described in Fig. 2 by continuous lines. *c)* $x(t)$ mimics an AM-FM HRV signal during stress testing: components are described in Fig. 2. Two hundred pairs $[x_1(t), x_2(t)]$ have been created, for each theoretical coherence level, from 0.1 to 0.95 in steps of 0.05. The bias is computed as the difference between the group average of the mean band coherence $\bar{\gamma}_B$ (computed, for every couple, over time) and the corresponding theoretical $\gamma_{0,B}$. Variability is assessed by estimating the group average of the standard deviation of $\bar{\gamma}_B$.

II) $\gamma_{0,B}(t)$ is time-varying, $x(t)$ is of type *Ic* (see Fig. 2): three different time evolutions of $\gamma_{0,B}(t)$ (*a, b* and *c*) are modeled and described by gray line in Fig. 4. In this cases, 1000 pairs $[x_1(t), x_2(t)]$ have been created and $\gamma_B(t)$ is estimated in mean and standard deviation over all realizations. The Simulation parameters are summarized in Table 1. Note that when $x(t)$ is a white noise (case *Ia*), $\gamma_B(t)$ represents a global (not localized in frequency) estimation, while in the other cases a localized band coherence estimation is performed. $F_{HF}(t)$ is included in the kernel design to estimate ν_0. Parameter a, λ and k are 0.01, 0.25 and 0.002 respectively.

Table 1. simulation parameters

	Ia	*Ib*	*Ic*	*II*
Type	T-inv	T-inv	T-inv	TV
$x(t)$	$\eta(t)$	resp	HRV	HRV
$B(t)$ [Hz]	2	$F_{HF}(t)\pm0.075$	$F_{HF}(t)\pm0.05$	$F_{HF}(t)\pm0.05$

2.5. Real data application

Real data application aims at tracking the autonomic response to orthostatic stress by estimating the TFC between HRV and SPV during tilt testing. Fifteen healthy subjects were involved in the test, consisting in 4 minutes of supine position (T_1), five minutes of tilting position at 70° (T_2) and other 5 minutes of recovering in supine position (T_3). From the ECG recording (sampling rate F_s=1 KHz), instantaneous HR was obtained using a method based on the integral pulse frequency modulation model [5]. Noninvasive blood pressure was recorded using a Finometer (F_s=250 Hz) and respiratory rate was estimated using a sensor belt (F_s=150 Hz). SP values were measured as the local maximum of the blood pressure signal within the RR intervals. All signals were resampled at 4 Hz. In the signal-dependent kernel design, the respiratory rate is used to approximate $F_{HF}(t)$ and parameter a, λ and k are 0.01, 0.25 and 0.002 respectively. Band coherences $\gamma_{LF}(t)$ and $\gamma_{HF}(t)$ were extracted by averaging $\gamma(t,f)$ in a spectral band $B(t)$ of 0.1 Hz centered around the maximum of the TF cross spectrum in LF [0.04:0.15] and HF [0.15:0.5] ranges.

3.   Results and discussion

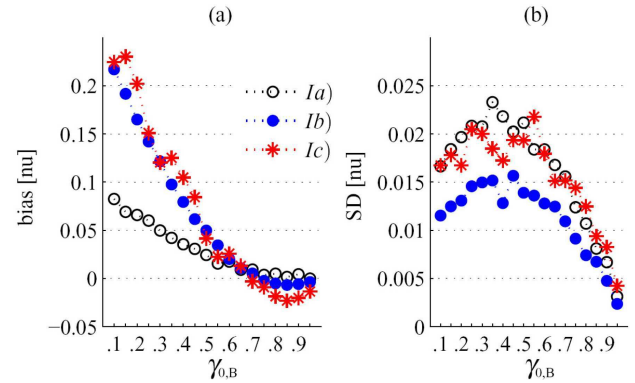## 3.1.   Simulation for assess accuracy

Figure 3. Type *I*: bias (a) and SD (b).

The methodology for estimating TFC has been tested in six different situations, using the signal-dependent QTFD described above. Results of case *I* and of case *II* are shown in Fig 3 and 4. In simulations of case *I*, bias is very low (< 0.05) for $\gamma_{0,B} > 0.5$, while standard deviation is always small. In simulations of case *II*, the estimator performs very well for gradual and slow coherence changes (Fig. 4a). In case of abrupt changes (Fig. 4b) the estimator takes few seconds to properly adjust to the new values, while when short decorrelating events appear (Fig 4c) the estimator is able to correctly localized them, even if with a higher bias. It is worth to note that better results could be achieved by manually adjusting the parameters of the smoothing kernel to each specific situation, but this requires a-priori knowledge of TF signals structure, which in real cases it is often not available.
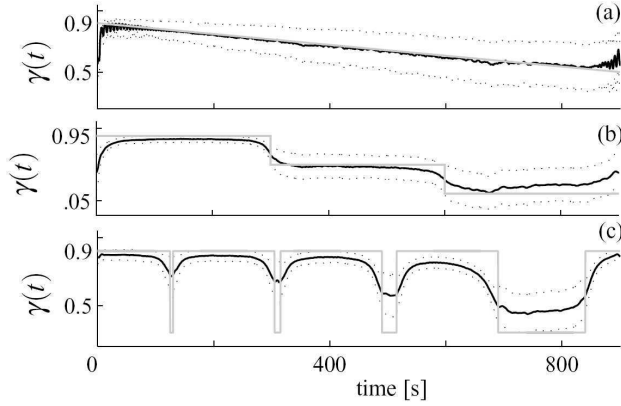
Figure 4. Type II: tracking capability. Gray lines: $\gamma_{0,\mathrm{B}}(t)$, black and dotted lines: mean trend $\pm$ SD of $\gamma_{\mathrm{B}}(t)$
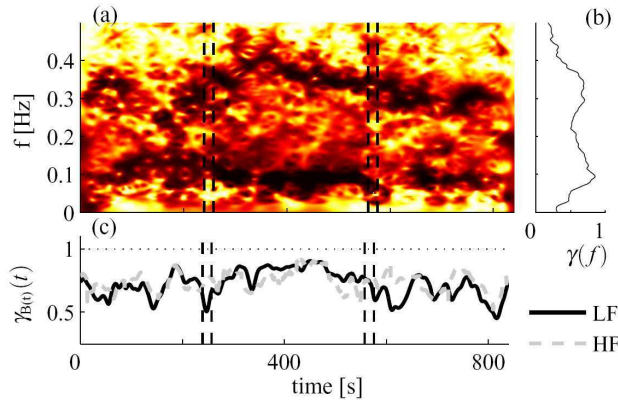

Figure 5. a): black $\gamma(t,f)=1$, white $\gamma(t,f)=0$; b): band coherences $\gamma_{\mathrm{LF}}(t)$ and $\gamma_{\mathrm{HF}}(t)$; c): $\gamma(f)$

3.2. Real application

In Fig 5, a representative example of $\gamma(t,f)$ estimation is shown. Vertical lines mark the tilting movement of the automatic bed, first upward (from T_1 to T_2) and then downward (from T_2 to T_3). During T_2 TFC is higher than during T_1 and T_3 indicating that, as response to orthostatic stress, the HRV-SPV linear coupling increases. This trend is observed in all subjects but one, being particularly clear in those subjects with low respiratory rate (< 0.2 Hz). The median trend, computed over the 15 subjects, of $\gamma_{\mathrm{HF}}(t)$ and $\gamma_{\mathrm{LF}}(t)$, is shown in Fig 6a and 6b, respectively. The changes in band coherence are evaluated comparing its median values, computed over time in T_1, T_2 and T_3: results of T Student's test are shown in table 2. During tilting, the TFC increase in LF is significant with respect to both T_1 and T_3. Bigger differences are observed between $\gamma_{\mathrm{LF}}(T_2)$ and $\gamma_{\mathrm{LF}}(T_3)$ than between $\gamma_{\mathrm{LF}}(T_1)$ and $\gamma_{\mathrm{LF}}(T_2)$. Statistical differences between $\gamma_{\mathrm{LF}}(T_1)$ and $\gamma_{\mathrm{LF}}(T_3)$ are not significant. In HF band, the median trend of TFC is slightly lower than in LF. A significant increase in $\gamma_{\mathrm{HF}}(t)$ is also observed during tilting.
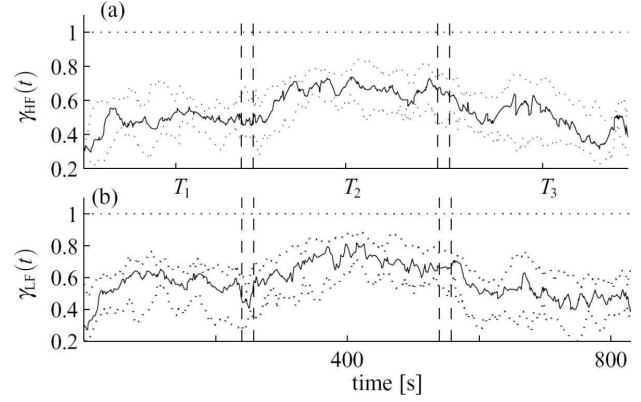

Figure 6. median trend of (a) $\gamma_{\mathrm{HF}}(t)$ and (b) $\gamma_{\mathrm{LF}}(t)$

Table 2. Statistical differences of $\gamma_{\mathrm{B}(t)}(t)$ [p-values]

$B(t)$	T_1-T_2	T_2-T_3	T_1-T_3
LF	0.02	0.001	0.28
HF	0.04	0.02	0.83

4.   Conclusion

In this communication a methodology for continuously quantifying the linear coupling of cardiovascular interactions using QTFD has been presented. Its reliability and robustness have been assessed quantifying bias, variability and tracking capability of the estimator in different physiological situations. An application aiming at tracking SPV-HRV coupling during orthostatic stress shows that during tilting TFC increases in both LF and HF band.

Acknowledgments

References

[1] Mainardi LT. On the quantification of heart rate variability spectral parameters using time-frequency and time-varying methods. Phil Trans R Soc A 2009;367(1887):255–275.
[2] Matz G, Hlawatsch F. Time-frequency coherence analysis of nonstationary random processes. In Proc. Tenth IEEE Workshop on Stat. Signal and Array Process. 2000; 554–558.
[3] Hlawatsch F. Duality and classification of bilinear time-frequency signal representations. IEEE Trans Signal Process 1991;1564–1574.
[4] Hlawatsch F, Flandrin P. The Wigner Distribution - theory and applications in signal processing. Elsevier, 1997; 59–113.
[5] Mateo J, Laguna P. Analysis of heart rate variability in the presence of ectopic beats using the heart timing signal. IEEE Trans Signal Process 2003;50:334–343.